ENGENHARIAS, TECNOLOGIA, GESTÃO E TURISMO
ENGINEERING, TECHNOLOGY, MANAGEMENT AND TOURISM
INGENIERÍA, TECNOLOGÍA, ADMINISTRACIÓN Y TURISMO

millenium

Millenium, 2(9), 13-23.

en

TENSÃO DE ADESÃO DE REVESTIMENTOS CERÂMICOS OBTIDOS POR PROJEÇÃO ROBÓTICA À CHAMA
ADHESION STRENGTH OF FLAME SPRAYED CERAMIC COATINGS OBTAINED BY ROBOTIC PROJECTION
TENSIÓN DE ADHESIÓN DE REVESTIMIENTOS CERÁMICOS OBTENIDOS POR PROYECCIÓN ROBÓTICA A LLAMA

Eurico Seabra[1]
Luís Silva[1]
Fuad Aliew[2]
Joana Morais Sarmento[1]

[1] Universidade do Minho, Departamento de Engenharia Mecânica, Guimarães, Portugal
[2] Gebze Technical University, Electronics Engineering Department, Istanbul, Turkey

Eurico Seabra - eseabra@dem.uminho.pt | Luís Silva - lffsilva@dem.uminho.pt | Fuad Aliew - faliew@gtu.edu.tr |
Joana Morais Sarmento - a68613@alunos.uminho.pt

Corresponding Author
Eurico Seabra
Universidade do Minho
Campus de Azurém
4800-058 Guimarães
eseabra@dem.uminho.pt

RECEIVED: 22th May, 2018
ACCEPTED: 05th February, 2019

RESUMO

Introdução: Uma das possíveis aplicações de barreiras térmicas cerâmicas é no revestimento de moldes permanentes para fundição. A capacidade do molde suportar temperaturas muito elevadas (até 1600 °C), devido ao estado líquido do ferro fundido, desempenha um papel crucial na seleção de materiais.

Objetivos: Este artigo apresenta e discute os resultados obtidos a partir de testes de projeção robótica à chama, com o objetivo de quantificar a influência de vários fatores da projeção à chama na tensão de adesão de revestimentos de Níquel-Alumínio-Molibdênio e Óxido de Zircónia. Na literatura não foi encontrada uma tensão mínima de adesão requerida para a aplicação de barreiras térmicas cerâmicas no revestimento de moldes permanentes para fundição, assim, no trabalho apresentado neste artigo, pretende-se obter seus valores considerando várias combinações de parâmetros de projeção e substratos.

Métodos: A determinação da tensão de adesão foi realizada de acordo com a norma ASTM C633-79 em que os provetes revestidos foram colados a contra-provetes de aço CK45 grenalhados, com uma cola à base de cianoacrilatos (LOCTITE 415). De seguida aplicou-se um peso de 100 N durante 3 minutos para a força de compressão promover o início da reação de polimerização dos cianoacrilatos e aguardou-se 24 horas para que a junta colada tivesse tempo de adquirir a resistência máxima (o suficiente para arrancar o revestimento do provete). Realizaram-se depois ensaios de tração à velocidade de 1 mm/min.

Resultados: Os principais parâmetros estudados foram o material do substrato, o ângulo de projeção e a temperatura de pré-aquecimento do substrato. A maior força de adesão para a projeção a 90° (média de 6,2 MPa) foi obtida com os provetes de ferro fundido com grafite esferoidal (SGCI) com uma temperatura de pré-aquecimento de 120 ° C. Para o pré-aquecimento de 90 °C e ângulo de projeção de 90°, foram os provetes de duralumínio (AlCu) e de latão que obtiveram as maiores forças de adesão (média de 4,5 MPa). A projeção a 65 ° origina a maior tensão de adesão em todos os materiais utilizados para o substrato, sendo o maior valor (média de 8,3 MPa) obtido pelo ferro fundido de grafite esferoidal.

Conclusões: Os resultados obtidos sugerem claramente que o material do substrato e a temperatura de pré-aquecimento influenciam fortemente a tensão de adesão. A análise das microestruturas dos revestimentos, utilizando microscopia ótica, comprova esta observação.

Palavras-chaves: Projeção térmica; Adesão de revestimentos; Caracterização morfológica; Robótica

ABSTRACT

Introduction: One of the possible applications of ceramic thermal barriers is in shells (permanent moulds – die casting). The moulds` capacity to support very high temperatures (up to 1600 °C) plays a crucial role in the selection of materials due to the liquid state of the cast iron.

Objectives: This paper presents and discusses the obtained results from robotic flame projection tests, carried out with the purpose to quantify the influence of several factors of flame sprayed in the adhesion strength of coatings of Nickel-Aluminium-Molybdenum and Zirconium Oxide. In literature a minimum adhesion strength was not found for the application of thermal ceramic barriers in the coating of permanent casting moulds, so in this work it is intended to obtain its values considering several combinations of projection parameters and substrates.

Methods: The determination of the adhesion strength was performed according to the standard ASTM C633-79 where the coated test specimens were glued to CK45 steel against-specimens with a cyanoacrylate glue (LOCTITE 415). A weight of 100 N was then applied for 3 minutes to promote the initiation of the polymerization reaction of the cyanoacrylates and a period of 24 hours was needed so the bonded glue could acquire its maximum strength (sufficient enough to tear off the coating of the specimen). Finally tensile tests were carried out at the speed of 1 mm/min.

Results: The main parameters studied are the material of the substrate, the projection angle and the substrate preheating temperature. The higher adhesion strength for the sprayed to 90° (average value of 6.2 MPa) was obtained by the specimens of spheroidal graphite cast iron (SGCI) with a preheating temperature of 120 °C. For the preheating of 90 °C and spray angle of 90° the aluminum-copper (AlCu) and brass specimens were the ones that obtained the higher adhesion strengths (average value of 4.5 MPa). The sprayed of 65° originates the higher adhesion strength in all the materials used for the substrate, being the highest value (average value of 8.3 MPa) obtained by the spheroidal graphite cast iron.

Conclusions: The results obtained clearly suggest that the substrate material and the preheating temperature strongly influence the adhesion strength. The analysis of the coatings microstructures, using optical microscopy, supports this observation.

Keywords: Thermal spray; Adhesion coatings; Morphologic characterization; Robotics

RESUMEN

Introducción: Una de las posibles aplicaciones de barreras térmicas cerámicas es en el revestimiento de moldes permanentes para fundición. La capacidad del molde para soportar temperaturas muy altas (hasta 1600 °C), debido al estado líquido del hierro fundido, desempeña un papel crucial en la selección de materiales.

Objetivos: Este artículo presenta y discute los resultados obtenidos a partir de pruebas de proyección robótica a la llama, con el objetivo de cuantificar la influencia de varios factores de la proyección a la llama en la resistencia a la adhesión de revestimientos de Niquel-Aluminio-Molibdeno y Óxido de Zirconia. En la literatura no se encontró una tensión mínima de adhesión requerida para la aplicación de barreras térmicas cerámicas en el revestimiento de moldes permanentes para fundición, así en el trabajo presentado en este artículo, se pretende obtener sus valores considerando varias combinaciones de parámetros de proyección y sustratos.

Métodos: La determinación de la tensión de adhesión se realizó de acuerdo con la norma ASTM C633-79 en la que se probaron las probetas revestidas a contra-probetas de acero CK45 gralladas, con un pegamento a base de cianoacrilatos (LOCTITE 415). A continuación se aplicó un peso de 100 N durante 3 minutos para la fuerza de compresión promover el inicio de la reacción de polimerización de los cianoacrilatos y se aguardó 24 horas, para que la junta adhesiva tuviera tiempo de adquirir la resistencia máxima (suficiente para arrancar el revestimiento de la probeta). Se realizaron después los ensayos de tracción a velocidad de 1 mm/min**.**

Resultados: Los principales parámetros estudiados son el material del sustrato, el ángulo de proyección y la temperatura de precalentamiento del sustrato. La mayor fuerza de adhesión para la proyección a 90° (media de 6,2 MPa) fue obtenida con las probetas de hierro fundido con grafito esferoidal (SGCI) con una temperatura de precalentamiento de 120 °C. Para el precalentamiento de 90 °C y ángulo de proyección de 90°, fueron las probetas de duraluminio (AlCu) y de latón que obtuvieron las mayores fuerzas de adhesión (media de 4,5 MPa). La proyección a 65° origina la mayor tensión de adhesión en todos los materiales utilizados para el sustrato, siendo el mayor valor (media de 8,3 MPa) obtenido por el hierro fundido de grafito esferoidal.

Conclusiones: Los resultados obtenidos sugieren claramente que el material del sustrato y la temperatura de precalentamiento influyen fuertemente en la fuerza de adhesión. El análisis de las microestructuras de los revestimientos, utilizando microscopia óptica, comprueba esta observación.

Palabras Clave: Proyección térmica; Adhesión de revestimientos; Caracterización morfológica; robótica

INTRODUCTION

In order to ensure a high performance of composite moulds, with ceramic coatings (permanent moulds – die casting), it is essential to optimize the robotic flame projection parameters to assure a coating with appropriate thickness and a good adhesion to the metallic substrate of the mould.

Thermal spraying using the heat from a chemical combustion is known as flame spraying. The spraying material, initially in the form of powder, rod, cord or wire, is heated by a flame spray gun (figure 1) that can be adapted to use several types of combustible gases, such as, acetylene, hydrogen, propane and natural gas. As the materials are heated, they change to a plastic or molten state, and are accelerated by a compressed gas. The sprayed particles impinge upon the substrate, they cool and build up, particle by particle, into a lamellar structure forming a coating (Mahood, 1990; Clare & Crawmer, 1987).

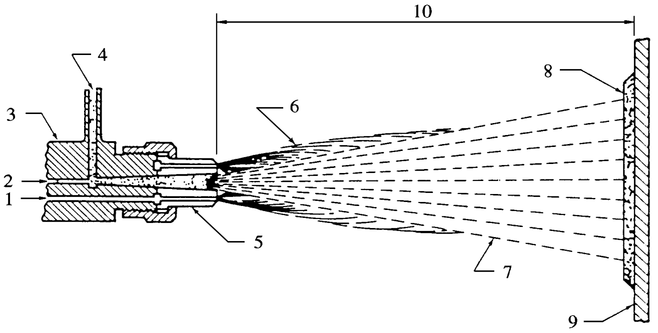

1 - Oxygen
2 - Fuel gas
3 - Gun
4 - Powder
5 - Nozzle
6 - Flame
7 - Spray stream
8 - Coating
9 - Substrate (material to coating)
10 - Spraying distance: 102-254 mm

Figure 1 - Cross section of a powder flame spray gun (Mahood, 1990)

The thickness proposed for the coating will be an important factor in the selection of the appropriate coating type, because the materials present distinguish properties to different thickness. Usually the properties intended for a coating that works as thermal barrier are (Vaßen et al., 2010; Vuoristo, 2014; Vijay & Balasubramanian, 2016; Dapkunas, 1997):

- Good adhesion to the substrate in order to support the residual stresses involved that can cause fissures and the destruction by lifting of the coating;
- Low thermal conductivity (to avoid the transfer of heat for the substrate);
- Proximity of the thermal expansion coefficients among the ceramic or metallic elements of the coating and the substrate material;
- Appropriate stability of the crystalline structure to the service temperatures;
- High reflectivity, and
- To be possible to repair the coating after it has been deteriorated in service.

The ceramic materials used in thermal barriers should be porous, not only to strongly reduce heat transfer (the air is bad conductor of heat), but also to improve the thermal shock resistance of the coating. These materials are based on oxides, cermets, nitrates, silicates, intermetallic compounds, some organic plastics and certain glasses. One of the materials commonly used in thermal barriers is the zirconium oxide (ZrO_2).

1. METHODS

ROBOTIC FLAME SPRAYING TESTS

The objective of the tests was to quantify the effect of several spraying parameters on the adhesion strength of ceramic coatings on metallic substrates typically used in moulds manufacture for cast iron foundry (permanent moulds – die casting). To achieve this objective, adequate substrate metallic alloys were selected to build permanent moulds; Nickel-Aluminum-Molybdenum was used for the bond coating and the Zirconium oxide for the coating, which can support very high temperatures (1600 °C) and its most appropriate to process cast iron. Using these materials several spraying flame tests were carried out and different coatings adhesions were obtained using the following variables:

- Material of the substrate - aluminum-copper (AlCu), spheroidal graphite cast iron (SGCI), brass, copper-chromium (CuCr) and ferritic grey cast iron (FGCI);
- Spray angle of 65° and 90°;
- Preheating temperature of 90 °C and 120 °C.

Thus, several spray flame tests were performed to cover specimens (prepared for adhesion strength tests of coatings whose drawing is shown in the figure 2) with bond coating and zirconium oxide. The area of the testing specimen to be coated corresponds to the diameter of 25 mm.

The flame spraying was made using a flame thermal spray robot type METCO AIR 2000 (trademark Mitsubishi), which has an articulate construction of six rotation axes with the intent to guarantee precision and repeatability of the displacement and positioning of the spray gun. The coated specimens were jointed to other identical specimens of steel, using cyanoacrylate glue. Later these assemblies were submitted to traction tests to determine the adhesion strength of the obtained coatings.

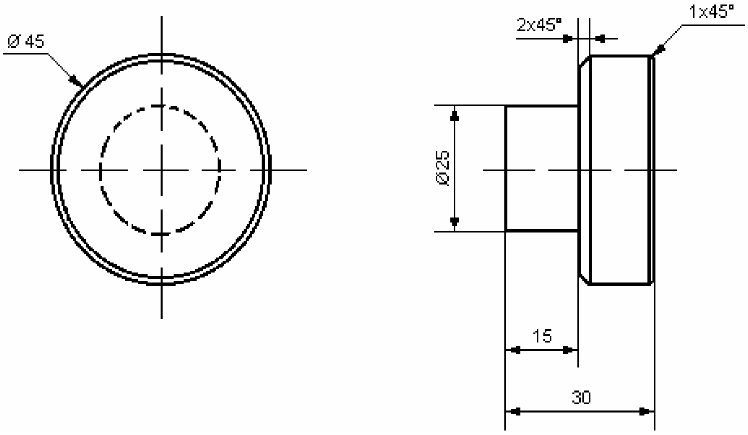

Figure 2 - Specimen used in the traction tests for the determination of the coating adhesion strength

Tables 1 and 2 list the main characteristics of the materials of the specimens (substrate) and of the sprayed powders, respectively.

Table 1 – Mechanical, chemical and physical properties of the five materials used as the substrate (Clarke & Phillpot, 2005; ASM, 1990a; ASM, 1990b, AMPCO, 1994)

Mechanical, chemistries and physics properties	AlCu	SGCI	Brass	CuCr	FGCI
Tensile strength [MPa]	427	600 - 800	414	494	300 - 400
Elastic tensile strength [MPa]	290	-----	138	446	-----
Elongation [%]	20	7 - 2	30	18	18 - 6
Macro hardness [HB10]	105	170 - 350	110	136	140 - 160
Thermal conductivity [W/mK]	134	50	123	322	46
Coefficient of thermal expansion [µm/mK]	65,1	13,6 (20-500°C)	20,9 (20-300°C)	17	13 (0-500°C)
Typical composition	Cu – 4,4% Si – 0,8% Mn – 0,8% Mg – 0,5% Remaining Al	--------	Cu - 57% Zn - 40% Pb - 3%	Cu –98,5% Cr – 1,1% others 0,5% Max.	C ≤ 2,3% 5,5% ≤ Si ≤ 7% 0,5% ≤ Mg ≤ 0,8%
Density [kg/m^3]	2700	7100	8200	8870	7300
Melting point [°C]	638	1120-1160	890	1230	1200

The experimental spraying tests were performed according to the following six phases:

1st Phase - Abrasive blasting of the specimen's surface

To obtain a coating with the required mechanical adhesion it is necessary to create a certain roughness in the substrate surface (Ra = 5 ± 1 µm) so the melted sprayed particles can adhere strongly. The increase of the roughness enhances the coating adhesion due to the following reasons (Mahood, 1990):

- Originates compressive tensions in the coating;
- Promotes the connection between the layers of the coating;
- Increases the connection surface;
- Decontaminate the surface.

Table 2 - Physical and chemical properties and respective spraying parameters of the used powders (AMPCO, 1982)

Spraying parameters and powders properties	Spraying powders	
	METCO 447NS (Mo-Ni-Al)	METCO 201NS (zirconium oxide)
Nozzle type of the Spray gun	K	K
Acetylene flow [l/min]	26,5	22
Oxygen flow [l/min]	42	30
Nitrogen flow[l/min]	6,9	6,9
Acetylene pressure [bar]	1,5	1,5
Oxygen pressure [bar]	4,5	4,5
Nitrogen pressure [bar]	5,5	5,5
Rotation speed of the powder feeder [rpm]	9,8	11,6
Spray rate [g/min]	34	30
Spray distance [mm]	140	75
Typical composition	Ni – 89,5% Al – 5,5% Mo - 5%	ZrO2 - 93% ; CaO - 5% Al2O3 – 0,5% ; SiO2 – 0,4% others – 1,1 %
Melting point [°C]	660	2535
Typical size range [µm]	+45 -88	+10 -53
Density [kg/m^3]	7200	5200
Porosity [%]	< 2	10
Powder weight per area of coating thickness of 0,1 mm [kg/m^2]	0,8	1,04
Coating weight per area of coating thickness of 0,1 mm [kg/m^2]	0,72	0,52
Deposition efficiency [%]	90	50

Spray gun velocity [m/min]	20	20

2nd Phase - Specimen's assembly in the spraying plate
Figure 3 depicts the assembly of the specimens in the spraying plate, showing also the relative positioning between the specimens of different materials.

3rd Phase - Robotic preheating with oxyacetylene flame
It is used with the purpose to reduce the residual stresses of the coatings obtained by flame spraying, due to the expansion that causes in the substrate. In addition, the preheating of the substrate does not allow that the water vapor product of the oxyacetylene combustion condenses in the surface, which can originate decreasing of the coating adhesion. The temperature used to preheat the substrate is about 100 °C (more precisely between 90 °C and 120°C) to guarantee that the surface will be always dry.

4th Phase - Robotic spraying of the bond coating (Nickel-Aluminum-Molybdenum)
This type of materials based in Nickel-Aluminum creates coatings with good adhesion because during flame spraying an exothermic reaction occurs among the aluminum and the nickel that brings additional heat to the process. Therefore it could be observed some local welding which increases the adhesion between the sprayed particles and the substrate (Vaßen, et al., 2010). Figure 3 also shows a phase of the robotic spraying of the bond coating.

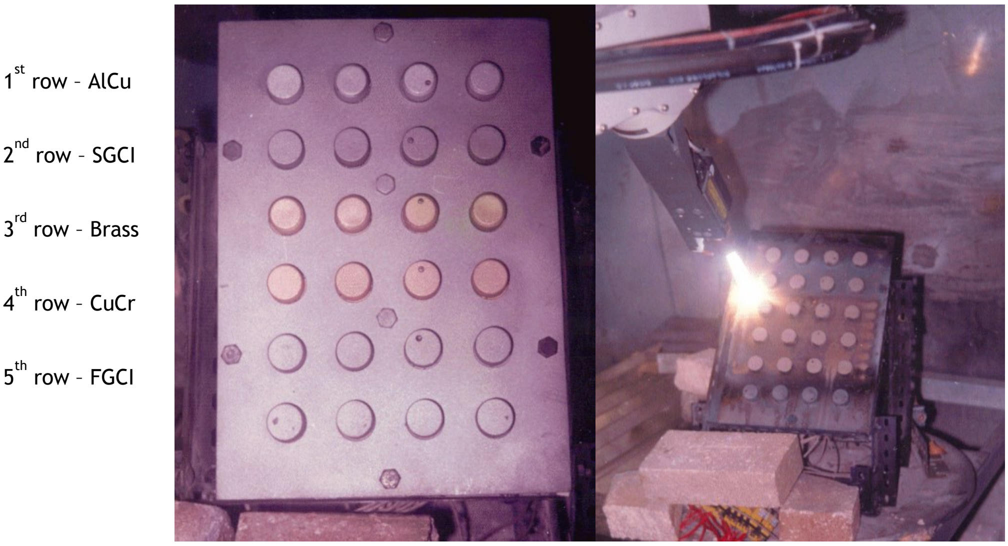

Figure 3 - Specimen's assembly in the spraying plate (on the left) and robotic spraying of the bond coating with a spray angle of 90° (on the right)

5th Phase - Robotic spraying of the zirconium oxide coating
The objective of the zirconium oxide spraying was to use a material that for its properties is considered a thermal barrier (Clarke & Phillpot, 2005). Figure 4 shows a phase of the robotic zirconium oxide spraying and the final appearance of the coating, composed by the bond coating and the zirconium oxide.

6th Phase - Adhesion strength according to the standard ASTM C633-79 (ASTM, 1989)
The coated specimens were joined using cyanoacrylate glue LOCTITE 415 (LOCTITE, 2010) to other identical specimens of steel CK45 (ASM, 1990a), whose contact surface was previously submitted to abrasive blasting to create a certain roughness to improve the glue adhesion.
To promote the beginning of the polymerization reaction of the cyanoacrylates it was necessary to apply a compressive force of 100 N in the assembly for a period of 3 minutes. Figure 5 shows, for each one of the five tested materials used for the substrate, four specimens assemblies that were submitted to tensile strength tests.

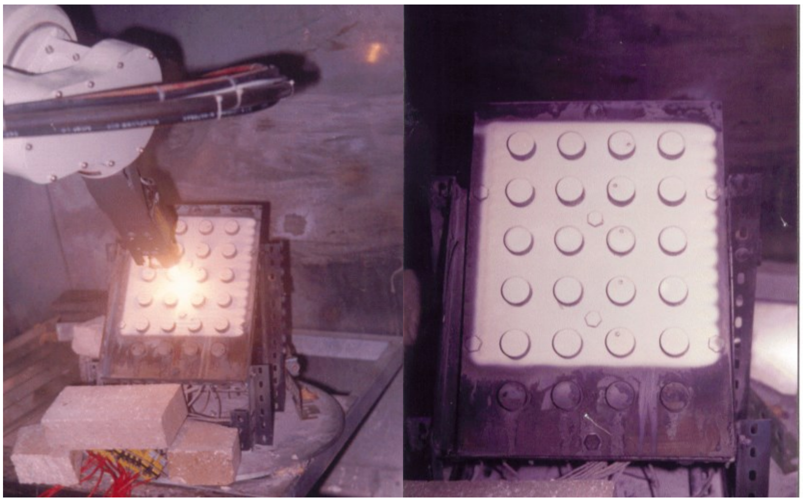

Figure 4 - Robotic spraying of the zirconium oxide coating with a spray angle of 90° (on the left) and final appearance of the coating (on the right)

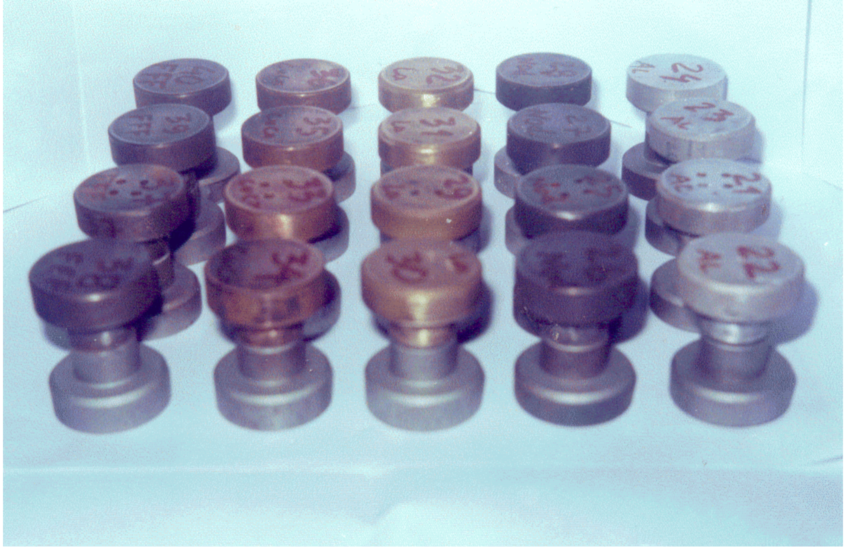

Figure 5 - Agglutinated assemblies of coated specimens with against-specimens (specimens on top)

After 24 hours, so that the agglutinated joint had time enough to achieve its maximum resistance (enough to pull the coating of the specimen), the traction tests were carried out using a testing speed of 1 mm/min (ASTM, 1989) to obtain the adhesion strength of the coating.

2. RESULTS AND DISCUSSION

Figure 6 shows the coating adhesion strength as a function of the material of the substrate for identical spraying parameters, namely spray angle and preheating temperature.

Figures 6a and 6b highlight the results for the robotic flame spraying tests carried out with a spray angle of 90°; they just differ in the preheating temperature, respectively, 120 °C and 90 °C. It can be concluded that for the spray angle of 90° the higher coating strength adhesion was obtained for the spheroidal graphite cast iron (SGCI) and copper-chromium (CuCr) specimens for the preheating temperature of 120 °C, while for preheating of 90 °C the aluminum-copper (AlCu) and brass specimens were the ones with an higher coating strength adhesion. Nevertheless it was not possible to formulate any conclusion for the ferritic grey cast iron (FGCI) specimens, because no spray flame tests were carried out with a preheating temperature of 120 °C.

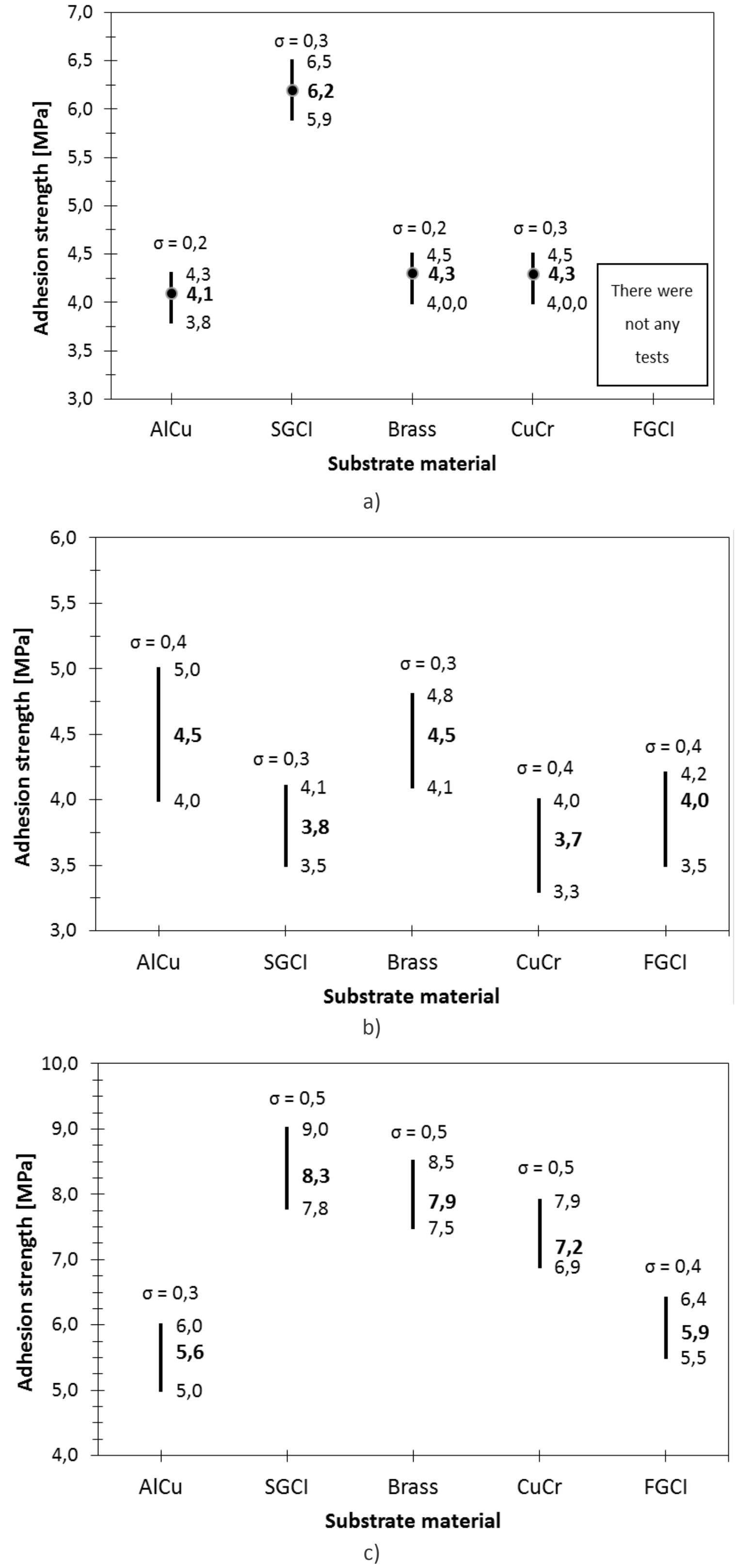

Figure 6 - Influence of the substrate material in the coating adhesion strength (maximum, minimum, average and standard deviation values): a) Spray angle of 90° and preheating temperature of 120 °C; b) Spray angle of 90° and preheating temperature of 90 °C and c) Spray angle of 65° and preheating temperature of 90 °C.

According to figures 6a and 6b, the higher adhesion strength for the spray angle of 90° was obtained for the specimens of spheroidal graphite cast iron (SGCI) with a preheating temperature of 120 °C (average of 6,2 MPa). For the preheating of 90 °C and a spray angle of 90°, the aluminum-copper (AlCu) and brass specimens were the ones that obtained the higher adhesion strengths (with an average of 4,5 MPa). Considering the spray angle of 90° and a preheating temperature of 120 °C, the aluminum-copper specimens obtained a smaller adhesion strength (average of 4,1 MPa) comparatively to the flame spray tests performed at 90 °C (average of 4,5 MPa). This can be caused by the fast oxidation of the hot aluminum-copper. The use of a low preheating temperature promotes a better adhesion of the coating because the surface will be less oxidized.

Considering figure 6c, which corresponds to a spray angle of 65° and to a preheating temperature of 90 °C, it is possible to observe that the spheroidal graphite cast iron (SGCI) and brass specimens obtained the highest values for adhesion strength (with an average of, respectively, 8,3 MPa and 7,9 MPa).

The differences determined for the adhesion strength of all the specimen materials considered can be justified by the predominant mechanical nature of the coating adhesion to the substrate. The spraying particles melt, flatten and conform to the roughness of the surface and they adhere mechanically amongst themselves and to the roughness of the substrate, implying that the coating presents an higher adhesion strength in substrates with better mechanical properties, namely, with an higher tensile strength.

Taking into consideration the adhesion strength values shown in the figure 6a (for a spray angle of 90° and a preheating temperature of 120 °C), it is observed that the spheroidal graphite cast iron (SGCI) presents the highest value (an average of 6,2 MPa), since it's the material that have the higher tensile strength (see table 1).

Considering the adhesion strength values shown in the figure 6b (for a spray angle of 90° and a preheating temperature of 90 °C), it is not clear why the spheroidal graphite cast iron does not present the highest adhesion strength value. Nevertheless it may occur due to the fact that the preheating temperature of 90 °C might not to be the most adequate for this material. However, this hypothesis is contradicted by the results presented in the figure 6c (for a spray angle of 65° and a preheating temperature of 90 °C), because it presents once again the higher adhesion strength (with an average value of 8,3 MPa); this fact led to the conclusion that something anomalous happened in the adhesion traction test of the spheroidal graphite cast iron specimens sprayed at 90° with a preheating temperature of 90 °C.

The spray angle of 65° shown in figure 6c originates the higher adhesion strength in all the materials used for the substrate, being the highest value (average of 8,3 MPa) obtained for the spheroidal graphite cast iron, proving to be the best material. It can also be concluded that the worst materials for the substrate are the ferritic grey cast iron (with an average value of 5,9 MPa) and the aluminum-copper (with an average value of 5,6 MPa), due to their low tensile strength.

To explain why the spray angle of 65° has an higher adhesion strength than the spray angle of 90°, these obtained coatings were analyzed using an optical microscope.

Figure 7 shows the bond coating (Nickel-Aluminum-Molybdenum) and the zirconium oxide in a brass substrate sprayed at 90°.

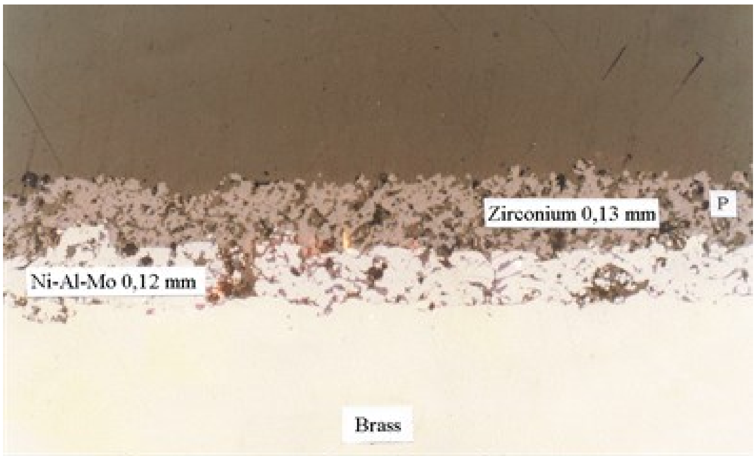

Figure 7 - Nickel-Aluminum-Molybdenum and zirconium oxide sprayed at 90° to a brass substrate (magnification: 100x)

According to figure 7, it can be concluded that the connection between the coating layers seems to be good because no fissures are observed. The bond coating as well as the zirconium oxide present little porosity (the darker points indicated by P in figure 7), however the zirconium oxide coating presents more porosity than the connection layer, since the zirconium oxide does not melt like the Nickel-Aluminum-Molybdenum. According to literature it is expected 10% of porosities in the zirconium oxide and less than 2% in the bond coating. On the other hand figure 8 shows the bond coating (Nickel-Aluminum-Molybdenum) and the zirconium oxide in a brass substrate sprayed at 65°.

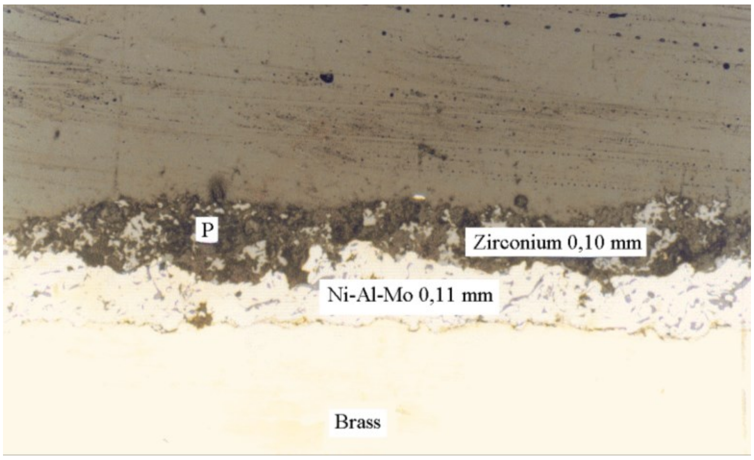

Figure 8 - Nickel-Aluminum-Molybdenum and zirconium oxide sprayed at 65° to a brass substrate (magnification: 100x)

Analyzing figure 8 it can also be concluded that the connection between the coating layers is again very good because no fissures are observed. The bond coating presents very little porosity (less than 2%) and the zirconium oxide coating presents again many darker points (indicated by P in figure 8). Nevertheless not all these darker points are due to porosity; many were created when polishing the sample for microscopic observation. The porosities were evaluated considering two different calculation methods: the first one was based on the calculation of the coating weight using the specific masses and characteristic porosities of its materials, and, the second one, using the microscopic observation of the coating. The porosity of the coatings obtained by the two tested spray angles (90° and 65°) are similar and correspond to the values stated by the manufacturer of the spraying materials, such as, bond coating (<2%) and zirconium oxide (10%).

The coatings produced with a spray angle of 65° obtained a less coating thickness than the ones sprayed at 90°. This is due to the smaller deposition efficiency of the spray at an angle of 65°. This fact was more evident in the zirconium oxide coating (with a decrease from 0,13 mm to 0,10 mm) than the one determined for the bond coating Ni-Al-Mo (with a decrease from 0,12 mm to 0,11 mm). Due to the thickness of the coatings in all substrates, the coatings sprayed at 65° produced larger adhesion strengths than the coatings sprayed at 90°.

As in other types of deposits, the coatings obtained by flame spraying contain residual stresses, which result from the contraction that occur during cooling and solidification of the sprayed materials (Gu et al., 2012; Karaoglanli, Dikici, & Kucuk, 2013; Xueling, Rong, & Wang, 2014). Those stresses are due to the individual contraction of the particles when they solidify in the substrate and its magnitude is proportional to the thickness of the coating. Due to this fact, the interface coating/substrate is submitted to shear tensions and only normal tensions are tolerated in the bond to obtain a good coating adhesion.

In addition, independently of the substrate used with different thermal conductivity and coefficient of thermal expansion, the coatings sprayed at 65° obtained higher adhesion strengths than the ones sprayed at 90°, because they are less thick and consequently have smaller residual stresses.

CONCLUSIONS

In this paper a study of the adhesion strength of flame sprayed ceramic coatings obtained by robotic projection is presented and discussed.

The deposition efficiency for all the sprayed materials reaches the maximum value with the spray angle of 90°, which enables the production of the largest coating thickness for the same processing time and spraying rate. The powders ceramics sprayed at 65° and 90° have similar porosities.

The coatings sprayed at 65° (with smaller thickness and with smaller residual stresses than the ones sprayed at 90°) have better adhesion strengths. The preheating temperature that promotes the best adhesion of the coating depends on the material of the substrate.

The coatings produced in less oxidized substrate materials present better adhesion strengths with higher preheating temperatures.

The use of substrates with good mechanical properties, such as tensile strength, is a major aspect that positively influences the value of the adhesion strength of coatings.

Seabra, E., Silva, L., Aliew, F. & Sarmento, J. M. (2019).
Adhesion strength of flame sprayed ceramic coatings obtained by robotic projection. *Millenium, 2*(9), 13-23.
DOI: https://doi.org/10.29352/mill0209.01.00177

REFERENCES

AMPCO (1982). METCO 447NS, METCO 201NS e METCO 105NS, Technical Bulletin - Flame Spray Equipment and Supplies, Ampco Metal Portugal Lda.

AMPCO (1994). METAL Technical Bulletin AMPCO 97, Ampco Metal Portugal Lda.

ASM (1990a). Handbook Committee Properties and Selection: Irons, Steels and High-Performance Alloys, Metals Handbook, Vol. 1, ASM, 10th ed., 244-247.

ASM (1990b). Handbook Committee Properties and Selection: Nonferrous Alloys and Special - Purpose Materials, Metals Handbook, Vol. 2, ASM, 10th ed., 175-207.

ASTM (1989). ASTM Standard Test Method for Adhesion or Cohesive Strength of Flame Sprayed Coatings C 633-79, Annual book of ASTM standards - Section 2, Nonferrous products, Metallic and inorganic coatings, metal powders, sintered P/M structural parts, Vol. 2.05, 633-667.

Clare, J. H., & Crawmer, D. E. (1987). Thermal Spray Coatings, Metals Handbook, Vol. 5 - Surface cleaning, Finishing and Coating, ASM, 9th ed., 361-374.

Clarke, D. R., & Phillpot, S. R. (2005). Thermal barrier coating materials, Materials Today, 8(6), 22-29.

Dapkunas, S. J. (1997). Measurement Methods and Standards for Processing and Application of Thermal Barrier Coatings, Journal of Thermal Spraying Technology, 1(1), 67-76.

Gu, L. J., Fan, X. Z., Zhao, Y., Zou, B. L., Wang, Y., Zhao, S. M., & Cao, X.Q. (2012). Influence of Ceramic Thickness on Residual Stress and Bonding Strength for Plasma Sprayed Duplex Thermal Barrier Coating on Aluminum Alloy, Surface Coating Technology Journal, 206(21), 4403-4410.

Karaoglanli, A. C., Dikici, H., & Kucuk, Y. (2013). Effects of Heat Treatment on Adhesion Strength of Thermal Barrier Coating Systems, Engineering Failure Analysis Journal, 32, 16-22.

LOCTITE (2010). Technical Data Sheet LOCTITE® 415™.

Mahood, E. R. (1990). Thermal Spraying - Practice, Theory, and Application, 1, 1-91.

Vaßen, R., Jarligo, M. O., Steinke, T., Mack, D. E., & Stöver, D. (2010). Overview on advanced thermal barrier coatings, The Journal of Surface and Coatings Technology, 205(4), 938-942.

Vijay, K., & Balasubramanian. K. (2016). Processing and design methodologies for advanced and novel thermal barrier coatings for engineering applications, Particuology Journal, 27, 1-28.

Vuoristo, P. (2014). Thermal Spray Coating Processes. Comprehensive Materials Processing Journal, 4, 229-276.

Xueling, F., Rong, X., Wang, T. J. (2014). Interfacial delamination of double-ceramic-layer thermal barrier coating system, Ceramics International Journal, 40(9), Part A, 13793-13802.